Sparse spectral unmixing for activity estimation in γ-RAY spectrometry applied to environmental measurements

Jiaxin Xu, Jerome Bobin, Anne de Vismes Ott, Christophe Bobin

Spectral unmixing for activity estimation in Gamma-Ray Spectrometry

Jiaxin Xu[1], Jérôme Bobin[2], Anne de de VISMES OTT[1] Christophe BOBIN[3]
[1]1RSN/PSE-ENV/SAME/LMRE
[2]CEA Saclay DRF/IRFU/DEDIP/LCS
[3]CEA/LIST/LNE/LNHB

A challenging problem in the domain of gamma-ray spectrum analysis is the rapid detection of artificial radionuclides, which are present at low activity levels. We introduce in this paper new algorithms for activity estimation based on spectral unmixing techniques, which aim to decompose a measured spectrum into individual spectra of radionuclides. We propose to tackle the activity estimation problem as an inverse problem, where individual activities appear as mixing weights related to individual spectra. In contrast to standard approaches, this allows us to account for the full spectrum of each radionuclide (i.e. peaks and Compton continuum). In this article, we investigate different approaches to solve the underlying spectral unmixing problem: standard regularized least squares regression (LS) and a novel regularized maximum likelihood estimation that allows to precisely account for the true Poisson statistics of the physical process underlying the detection. Both methods implement the non-negativity constraint to enforce the fact that the activity of radionuclides cannot be negative. Experimental results on simulated and measured spectra are presented and compared to standard methods, it is shown that the proposed approach leads to more accurate estimations, especially when the counting rate is low, which gives a significant advantage for the rapid detection.

***Index Terms*—gamma-ray spectrometry, spectral unmixing, inverse problem.**

I. Introduction

GAMMA-RAY spectrometry is one of the main technics used for measuring the activity concentrations of radionuclides in environmental samples because it is direct, non-destructive, rapid and multi-elementary. It particularly plays a central role to monitor the radiological environment or perform radioecology studies, which are some of the goals of The French Institute for Radiation Protection and Nuclear Safety (IRSN)[1]. More precisely, radioactivity in environmental samples is measured in the laboratory of environmental radioactivity metrology (LMRE), which is in charge of emergency preparedness. This task mandates the rapid measurements in case of an incident or an accident with releases so as to give rapid and reliable information to the population, as described in [1].

In this context, a gamma-ray spectrum is the histogram of the number of detected events as a function of the energy deposited by the gamma-ray or X-ray in the detector. Due to the possible interactions between photons and the material of the detector (see for instance [2] for more details). The spectrum obtained for one photon has two main components: a peak at the photon energy, called total absorption peak, and a continuum at lower energy, called Compton continuum. Depending on its decay scheme, a radionuclide can emit several photons and its individual spectrum thus comprises several peaks and associated continua. Finally the spectrum obtained with the measurement of an environmental sample (by HPGe detector) as shown in Figure 1 is the sum of the individual spectra of each radionuclide and the background spectrum. Radionuclides are classically identified thanks to their characteristic peak energy and quantified from the peak surface related to the activity via the detection efficiency.

We introduce a novel spectral unmixing algorithm that precisely take into account the exact Poisson statistics of the measured spectra. More precisely, spectral unmixing can be regarded as an inverse problem where a given gamma spectrum is composed of M channels:

$$\boldsymbol{x} = [x_1, ...x_M] \tag{1}$$

For $\forall i \in M$, the Poisson process of radioactive decay leads us to model the problem as:

$$x_i \sim \mathcal{P}([\boldsymbol{\Phi a}]_i + b_i) \tag{2}$$

We note the spectral signatures of each radionuclide with $\boldsymbol{\Phi} = [\boldsymbol{\phi}_1, ...\boldsymbol{\phi}_N]$ and $\boldsymbol{a} = [a_1, ...a_N]$ for their mixing weights, where N is the number of radionuclides. In (2), $[\boldsymbol{\Phi a}]_i$ is the sum of the counting rates for each radionuclide on the ith channel. Similarly, b_i stands for the counting rate of background spectrum on the ith channel. The aim is to decompose the measurement $\boldsymbol{x}$ into individual spectra of radionuclides and the background spectrum $\boldsymbol{b}$ (see Figure 1). The spectral signatures $\boldsymbol{\Phi}$ and a background spectrum $\boldsymbol{b}$ being known in advance, the activity estimation problem is therefore equivalent to finding the mixing weights $\boldsymbol{a}$.

A well-known challenge of the gamma-ray spectral analysis is the low statistics of the counting rate, which has attracted more attention in the field of rapid detection and rapid characterization of sources under emergency conditions. For example, the ^{137}Cs is an artificial radionuclide present in environmental samples in France. In practice, the detection of ^{137}Cs takes more than a week after the sampling. The objective of this study is to improve the gamma-ray spectral analysis and focus particularly on the artificial radionuclides at low statistics.

[1]https://www.irsn.fr/EN/Pages/home.aspx

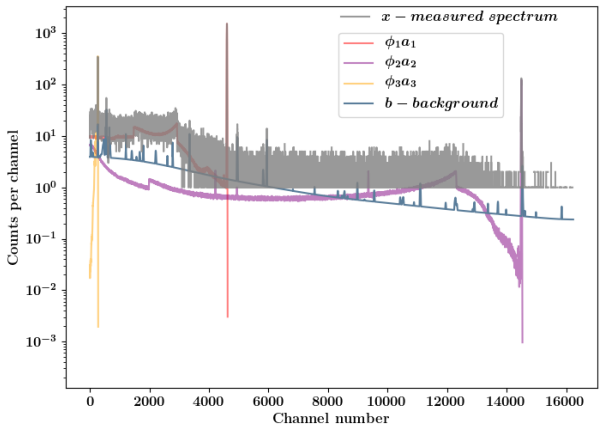

Fig. 1: Gamma-ray spectrum model

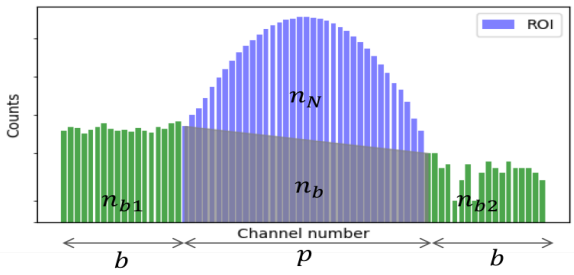

Fig. 2: Calculation of net area

A. State of the art

A common strategy used to analyze gamma-ray spectrum is the peak area calculation. For example, Genie2000 from Canberra is a commercial software based on a step of peak research followed by a Gaussian fit to get the peak surface. This process is usually based on Region of interest (ROI) as described in [3].

As shown in Figure 2, the net area n_N is calculated by correcting from the background with:

$$n_b = \frac{p}{2b}(n_{b1} + n_{b2}) \tag{3}$$

The performance of this approach is limited. Firstly, the calculation of net areas considers the counting distribution is approximately Gaussian, which is not valid at low statistics since an radioactive source emits photons randomly according to Poisson process. Secondly, a gamma-ray spectrum consists of photon-peaks and Compton continua, the problem of interference between individual spectra is difficult to handle with this peak-based analysis.

Peak-based analysis is a popular approach that has been implemented [4] to further account for the exact Poisson statistics of the measurements. However, this technique only relies on region of interest at the vicinity of related peaks and does not take into account the entire spectrum. [4] however shows the benefit of taking care of the Poisson statistics. The application of full-spectrum analysis of gamma-ray spectrum [5] uses re-weighted least squares for spectral unmixing of gamma-ray spectra. In this article, the authors demonstrated that compared to the standard peak-based analysis, using the full spectrum improves the sensitivity and reduces the time of measurement.

Activity estimation problem in gamma-ray spectrometry has been also studied in [6], which considers activity estimation as a sparse regression problem. In this article, the authors propose to estimate the number of individual electrical pulses and their arrival times. Other contributions of the activity estimation in the field of machine learning algorithms were also applied to gamma-ray spectral analysis as presented in [7], where peak energy data are applied to neural networks. In [8], the measured spectra are used to anomaly detection in gamma-ray spectra. However, approaches based on neural networks do not allow to precisely account the physical model underlying the detection.

B. Contribution

In this paper, we investigate a new approach for the estimation of the activity of radionuclides from gamma-ray spectra. The proposed approach relies on spectral unmixing techniques, which have been introduced independently in the field of remote sensing and hyperspectral imaging [9], [10]. In contrast to peak-based algorithms, spectral unmixing allows to make profit of the full spectrum of each radionuclide (i.e. peaks and Compton continuum). Accounting for all the information carried out by the spectrum should allow to improve activity estimation by lowering interferences between radionuclides'spectra.

The paper is organized as follows: Section II explores the use of unmixing algorithms for radioactivity estimation. To this end, two approaches are evaluated: i) a standard regularized least-squares estimator and ii) a novel regularized maximum Poisson likelihood estimator. In Section III, spectral unmixing is applied to simulated spectra, where we evaluate the estimation performance of the proposed algorithms. Comparisons are carried out with standard methods. Next, experimental results on real spectra are presented in Section IV. Section V provides conclusions and perspectives of this work.

II. Activity estimation algorithms

In this section, we study algorithms for activity estimation in gamma-ray spectrometry. Recall the model described in (2), we formulate the linear combination of each individual spectrum in the following matrix form:

$$\boldsymbol{y} = \boldsymbol{\Phi a} + \boldsymbol{b} \tag{4}$$

The mixing weights $\boldsymbol{a}$ is an array with non-negative entries, which is a property that will be enforced in the unmixing process. The estimation of $\boldsymbol{a}$ from a measured spectrum $\boldsymbol{x}$ can be addressed by minimizing a distance between $\boldsymbol{x}$ and the model $\boldsymbol{y}$. For that purpose, we investigate two different approaches: a standard least squares approach and a new Poisson statistics-based method.

A. Least squares unmixing algorithm

Spectral unmixing can be tackled as a standard regression problem. In this context, a classical approach consists in finding the solution $\boldsymbol{a}$ that minimizes the least squares error:

$$\hat{\boldsymbol{a}}_{LS} \in \underset{\boldsymbol{a}\geq 0}{\operatorname{argmin}} \frac{1}{2}\|\boldsymbol{\Phi a}+\boldsymbol{b}-\boldsymbol{x}\|_2^2 \tag{5}$$

Because of the non-negativity constraint, there is no closed-form expression for this problem. However, it can be recast as a generic inverse problem of the form:

$$\hat{\boldsymbol{a}} \in \underset{\boldsymbol{a}}{\operatorname{argmin}}\, f(\boldsymbol{a})+g(\boldsymbol{a}) \tag{6}$$

In the present unmixing problem, this can be recast as:

$$\hat{\boldsymbol{a}}_{LS} \in \underset{\boldsymbol{a}}{\operatorname{argmin}}\, i._{\boldsymbol{a}\geq 0} + \frac{1}{2}\|\boldsymbol{\Phi a}+\boldsymbol{b}-\boldsymbol{x}\|_2^2$$

where the regularization term $i._{\boldsymbol{A}\geq 0}$ is the characteristic function of the convex set (*i.e. non-negative orthant*) $\{\boldsymbol{a}\geq 0\}$. It is precisely defined as follows:

$$i._{\boldsymbol{a}\geq 0} = \begin{cases} 0, \text{if } \boldsymbol{a}\geq 0 \\ \infty, \text{otherwise} \end{cases} \tag{7}$$

Since this function is non-differentiable, solving the problem in (5) cannot be performed with standard gradient descent algorithms but requires the use of recently introduced proximal algorithms [11]. In brief, one can tackle this optimization problem with the Forward-Backward splitting (FBS) algorithm [12] since it verifies the following properties:

- The fidelity term is differentiable, and its gradient is defined as:

  $$\nabla f(\boldsymbol{a}) = \boldsymbol{\Phi}^T(\boldsymbol{\Phi a}+\boldsymbol{b}-\boldsymbol{x})$$

  Furthermore, the above gradient is Lipschitz with constant $L = \|\boldsymbol{\Phi}^T\boldsymbol{\Phi}\|_2$, where $\|\,.\,\|_2$ stands for the spectral norm of a matrix (*i.e.* its largest eigenvalue).
- The regularization term is convex and admits a proximal operator [11], which is generically defined as:

  $$\text{prox}_g(x) = \underset{y}{\operatorname{argmin}}\, g(y)+\frac{1}{2}\|y-x\|_2^2 \tag{8}$$

  The proximal operator of the non-negativity constraint (7) is simply defined as the orthogonal projection onto the non-negative orthant:

  $$\text{prox} i._{\boldsymbol{a}\geq 0} = \begin{cases} 0, \text{if } \boldsymbol{a}<0 \\ \boldsymbol{a}, \text{otherwise} \end{cases} \tag{9}$$

In the sequel, we make use of an accelerated version of the FBS algorithm coined FISTA [13]. The algorithm is summarized in Algorithm 1. This algorithm is guaranteed to converge to the unique minimum of (5) when the gradient step $\gamma \leq 1/L$. In practice, the algorithms stops when the relative variation of $\boldsymbol{a}$ between two consecutive iterations is lower than 10^{-12}.

Algorithm 1 Pseudocode of FISTA with constant stepsize

Input:
Fix the step size $0<\gamma<1/\|\boldsymbol{\Phi}^T\boldsymbol{\Phi}\|_2$
Fix the number of iterations: k_{max}
Initialization:
$\boldsymbol{a}^0=0$, $t^1=1$, $\boldsymbol{a}_y^1=\boldsymbol{a}^0$
while $k<k_{max}$ **do**
  $\boldsymbol{a}^k = \text{prox}\; i._{\boldsymbol{a}\geq 0}\left(\boldsymbol{a}_y^k - \gamma\boldsymbol{\Phi}^T(\boldsymbol{\Phi a}_y^k+\boldsymbol{b}-\boldsymbol{x})\right)$
  $t_{k+1} = \frac{1+\sqrt{1+4t_k^2}}{2}$
  $\boldsymbol{a}_y^{k+1} = \boldsymbol{a}^k + \left(\frac{t_k-1}{t_{k+1}}\right)(\boldsymbol{a}^k-\boldsymbol{a}^{k-1})$
end while

B. Poisson unmixing algorithm

From a statistical perspective, the least squares approach is equivalent to a maximum likelihood estimate assuming that the underlying noise is additive, white and Gaussian. To further account for the precise Poisson statistics of the spectroscopic measurement, we introduce a novel estimator that combines the maximization of the likelihood related to the Poisson statistics along with the non-negativity of the activities to be estimated. Therefore the probability of a given energy channel i to measure x_i counts is given by:

$$\mathcal{P}\left(X_i = x_i \middle| [\boldsymbol{\Phi a}]_i + b_i\right) = \frac{\lambda_i^{x_i}e^{-\lambda_i}}{x_i!} \tag{10}$$

where $\lambda_i = [\boldsymbol{\Phi a}]_i + b_i$. Thanks to the statistical independence of each channel, the joint probability or likelihood for the different channels is then given by:

$$\mathcal{P}\left(\boldsymbol{X}=\boldsymbol{x}\middle|\boldsymbol{\Phi a}+\boldsymbol{b}\right) = \prod_i \frac{\lambda_i^{x_i}e^{-\lambda_i}}{x_i!} \tag{11}$$

Maximizing the likelihood is equivalent to minimizing the neg-log-likehood, which leads to the following Poisson statistics-based activity estimator:

$$\hat{\boldsymbol{a}}_{Poisson} \in \underset{\boldsymbol{a}\geq 0}{\operatorname{argmin}} \sum_i [\boldsymbol{\Phi a}]_i + b_i - x_i \log\left([\boldsymbol{\Phi a}]_i + b_i\right) \tag{12}$$

which can be recast in the following vector formulation:

$$\hat{\boldsymbol{a}}_{Poisson} \in \underset{\boldsymbol{a}\geq 0}{\operatorname{argmin}}\, \boldsymbol{\Phi a}+\boldsymbol{b}-\boldsymbol{x}\odot\log\left(\boldsymbol{\Phi a}+\boldsymbol{b}\right)$$

where $\odot$ is the Hadamard product.
In contrast to the optimization problem that defines the least squares estimator, the above minimization problem cannot be solved with the FBS algorithm since none of the two terms is differentiable. Fortunately, both terms admit a proximal operator, which makes the application of first-order primal-dual algorithms such as the Chambolle-Pock (CP - see [14]) algorithm possible. The description of the CP algorithm to compute $\hat{\boldsymbol{a}}_{Poisson}$ is given in Algorithm 2. In this pseudo-code, as defined in (8), the proximal operator of the neg-log-likelihood f of the joint Poisson distribution of the measurements is:

$$prox_{\lambda f}(\boldsymbol{y}) = \frac{\boldsymbol{y}+\boldsymbol{b}-\lambda+\sqrt{(\lambda-\boldsymbol{y}-\boldsymbol{b})^2+4\lambda\boldsymbol{x}}}{2} - \boldsymbol{b} \tag{13}$$

Algorithm 2 Pseudocode of chambolle-pock algorithm

Input:
Fix the parameters: $\sigma, \tau > 0$ and $\sigma\tau < 1/\|\mathbf{\Phi}^T\mathbf{\Phi}\|_2$.
Fix the number of iterations: k_{max}
Initialization:
$\boldsymbol{a}^0 = 0$, $\bar{\boldsymbol{a}}^0 = \boldsymbol{a}^0$, $\boldsymbol{u}^0 = \mathbf{\Phi}\boldsymbol{a}^0$
while $k < k_{max}$ **do**

$$v = u^{(k)} + \sigma\mathbf{\Phi}\bar{\boldsymbol{a}}^{(k)}$$

$$u^{(k+1)} = v - \sigma \text{ prox }_{(1/\sigma)f}\left(\frac{v}{\sigma}\right)$$

$$\boldsymbol{a}^{(k+1)} = \text{prox }_{i_{\cdot \boldsymbol{a}\geq 0}}\left(\boldsymbol{a}^{(k)} - \tau\mathbf{\Phi}^T u^{(k+1)}\right)$$

$$\bar{\boldsymbol{a}}^{(k+1)} = \boldsymbol{a}^{(k+1)} + \theta(\boldsymbol{a}^{(k+1)} - \boldsymbol{a}^{(k)})$$

end while

where $\boldsymbol{x}$ and $\boldsymbol{b}$ stand for the measured spectrum and the background spectrum. Similarly to the FBS algorithm, the convergence of the CP algorithm is ensured to convergence $\sigma\tau < 1/\|\mathbf{\Phi}^T\mathbf{\Phi}\|_2$ and $\theta = 1$. The step parameters σ and τ are chosen with $\sigma = 10^{-4} \rightarrow 10^{-3}$ and $\tau = 0.9/(\sigma * L)$ for a better convergence rate. The choice of σ is related to the total number of counts in the mesured spectrum. $\sigma = 10^{-4} \rightarrow 10^{-3}$ is suitable for simulated spectra and real spectra that we used in this work. The stop criterion of the algorithm is as the FBS algorithm with relative variations of $\boldsymbol{a}$ lower than 10^{-12}.

III. Numerical evaluation on synthetic data

In this section, we evaluate the estimation performance of the proposed algorithms with simulated gamma-ray spectra. In contrast to standard unmixing problems that involve additive Gaussian noise, the Poisson nature of the measurements' statistics makes it highly dependent on the actual mixing. In the context of gamma-ray spectrometry, the ability to estimate precisely the mixing weight of a given radionuclide will therefore strongly depend on the contribution of the others. To further highlight the performances of the unmixing methods, the following mixing scenarios are investigated:

- Case 1: we consider the mixture of 2 radioactive sources with different energies: 200 keV and 500 keV, 1000 keV and 500 keV. In this case, it will be possible to assess the impact of the Compton contribution of a given radionuclide on the determination of another radionuclide.

- Case 2: we investigate a typical routine aerosol filter sample with 5 radionuclides: ^{7}Be , ^{22}Na ,^{40}K ,^{137}Cs ,^{210}Pb. The mixing weights are fixed to customarily observed values. In this test, we further evaluate the ability to estimate the level of a low-activity artificial radionuclide such as ^{137}Cs for different total count numbers.

A. Description of the simulations

Each individual spectral signature of radioactive sources is defined by its radioactive decay process and the detection efficiency of the measurement, depending on the detector and the counting geometry. In this work, the simulations are performed with the Monte Carlo N-particle (MCNP) Transport Code, a software package for simulating radiation transport developed by Los Alamos National Laboratory [15]. The sample-detector configurations are simulated for a HPGe detector (60 percent of relative efficiency) and a 60 mL cylindrical counting geometry.
For case 1, the spectral signatures of sources with specific energies are simulated with MCNPX (MCNP eXtended). For case 2, the simulations are composed of mixtures of realistic spectral signatures of radionuclides. We make use of MCNP-CP (A Correlated Particle Radiation Source Extension of a General Purpose Monte Carlo N-Particle Transport Code) [16] to compute their individual spectral signatures. It simulates physics of nuclear decay and the subsequent emissions.

B. Experiments on the combination of two radioactive sources

We consider the mixture of two radioactive sources at 500 keV, noted $\boldsymbol{\phi}_1$, and 200 keV/1000 keV, noted $\boldsymbol{\phi}_2$. The measured spectra are defined as follows:

$$\boldsymbol{x} \sim \mathcal{P}(\boldsymbol{\phi_1}a_1 + \boldsymbol{\phi_2}a_2 + \boldsymbol{b}) \tag{14}$$

where a_1 and a_2 stand for the individual activities (mixing weights) of the sources. $\boldsymbol{b}$ is the spectrum of the background radiation. As shown in Figure 3-a and Figure 3-b, we generate simulations as follows: $\boldsymbol{a}_1$ for source 500 keV kept fixed and we change $\boldsymbol{a}_2$ for 200 keV/1000 keV. Next, we simulate 30 gamma-ray spectra for each linear combination level by random Poisson process as described in (14).
In order to compare the performance of the algorithms to those of spectral analysis based on the calculation of peak areas, we perform a peak area determination process according to algorithms discussed in [3]. For comparison purposes, it should be noted that the mixing weight is not a good measure for quantifying the activity levels of different sources due to the different Compton continuum levels of source 200 keV and 1000 keV. One way to overcome this problem is to use the net area (defined in [3]) of the peaks associated to radioactive sources, this is done by converting the estimated mixing weights into net areas of peaks respectively.
The performances of these three estimators are compared in Figure 3, the first column for mixtures of 500keV and 200 keV, the second column for mixtures of 500keV and 1000 keV. Error bars are computed based on Monte Carlo simulations with relative error defined by $\frac{\|a-\hat{a}\|}{\|a\|}$. The median values and confidence intervals between percentile 25 and percentile 75 are displayed.

Results

- The estimated values obtained with the three estimators are compared to the real simulated values in Figure 3-c,d for source 500 keV and Figure 3-g,h for source 200 keV/1000 keV. The confidence intervals between percentile 25 and percentile 75 of each estimator show that, the Poisson unmixing yields lower uncertainty compared to least squares unmixing and peak-based

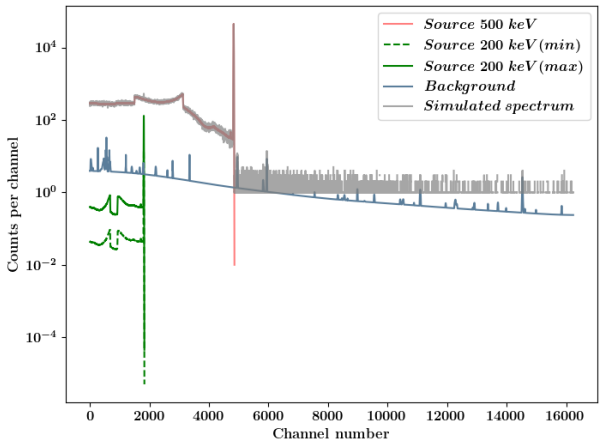

(a) Mixture of radioactive source 500 keV and 200 keV

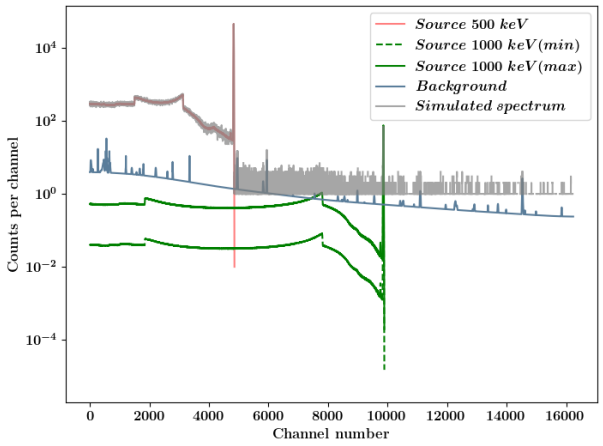

(b) Mixture of radioactive source 500 keV and 1000 keV

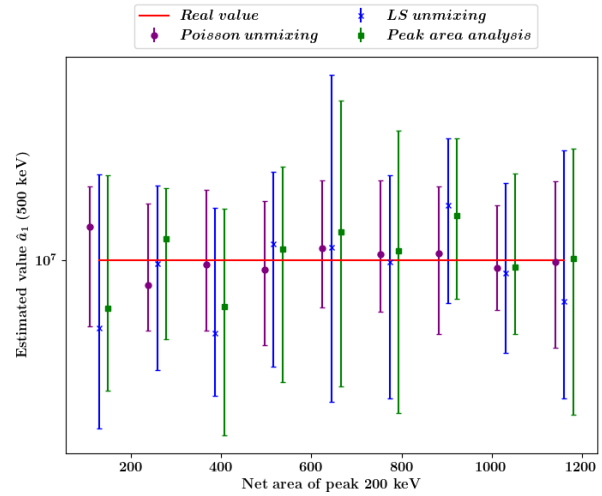

(c) Estimation of source 500 keV (mixed with 200 keV)

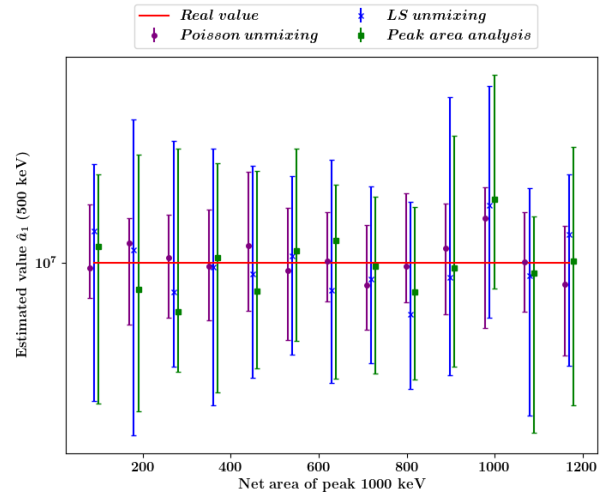

(d) Estimation of source 500 keV (mixed with 1000 keV)

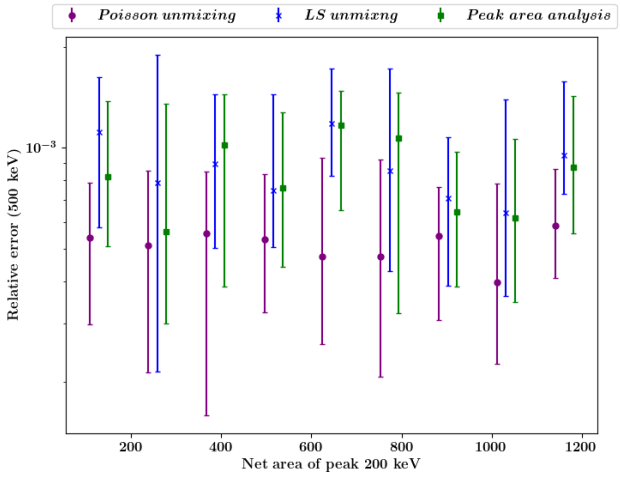

(e) Estimation relative error of source 500 keV (mixed with 200 keV)

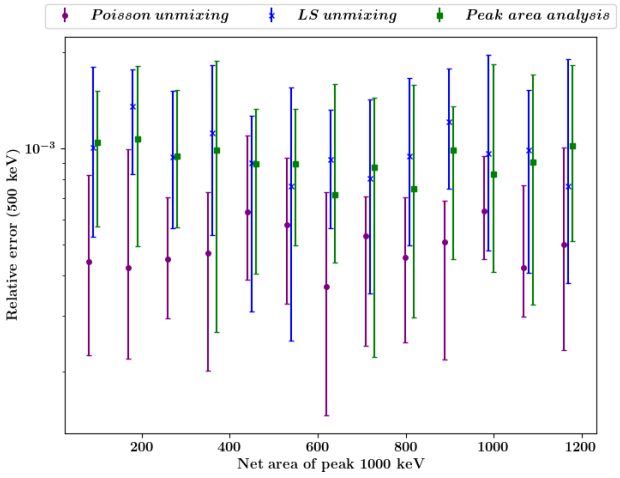

(f) Estimation relative error of source 500 keV (mixed with 1000 keV)

analysis. For further quantitative accuracy analysis, the relative error bars of each estimator are illustrated in Figure 3-e,f for source 500 keV and Figure 3-i,j for source 200 keV/1000 keV. It has to be pointed out that,

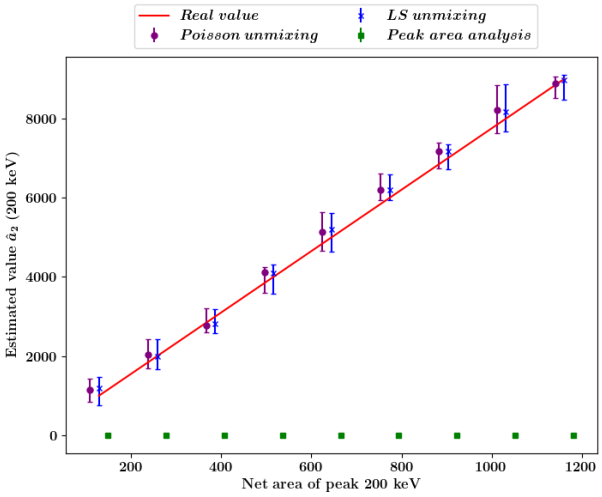

(g) Estimation of source 200 keV

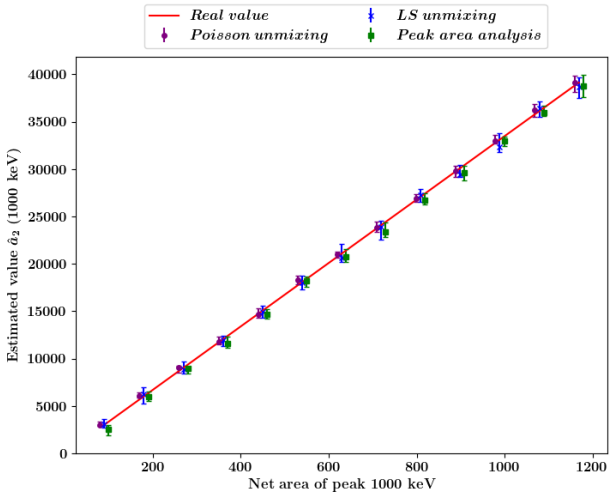

(h) Estimation of source 1000 keV

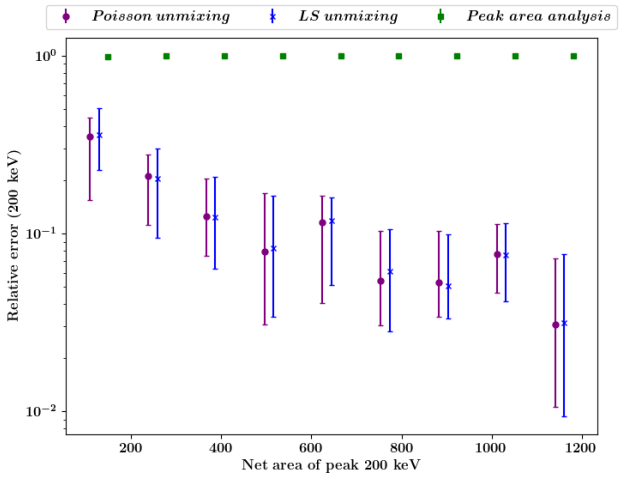

(i) Estimation relative error of source 200 keV

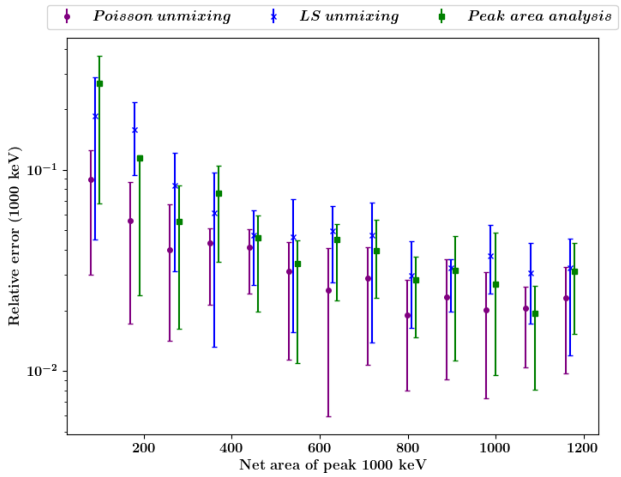

(j) Estimation relative error of source 1000 keV

Fig. 3: (a) (b) show the linear combination model of mixtures of 500 keV and 200/1000 keV. (c) (d) Illustration of estimated values for source 500 keV. (e) (f) with respect to relative errors comparison purpose for source 500 keV. (g) (h) Illustration of estimated values for source 200/1000 keV. (i) (j) with respect to relative errors comparison purpose for source 200/1000 keV. The results are plotted as a function of the net areas of 200/1000 keV.

the Poisson unmixing provides more accurate estimations with lower uncertainty.

- The results show that the estimation performance of each algorithm improves when the radioactivity level increases (see the evolution of estimation relative error for source 200 keV and 1000 keV in Figure 3-i,j). Compared to the source 500 keV, we get larger relative errors for 200 keV/1000 keV with low couting rate. This confirms again the limitation in low activity measurements.

- The peak-based analysis cannot detect the source of 200 keV (see Figure 3-g), however, it can be detected in the case of 1000 keV (Figure 3-f). We can conclude that, comparing to the estimator considering only the peak, the proposed spectral unmixing estimators using the full spectrum improves the estimation performance, which provides significant benefits when the peak of a source is located under the continuum of other sources.

C. Realistic simulations of routine aerosol samples

The comparisons are carried out on simulated spectra that are composed of 5 radionuclides: ^{7}Be, ^{22}Na, ^{40}K, ^{137}Cs, ^{210}Pb. These 5 radionuclides are the most commonly found in standard aerosol samples. The level of counting rate of each radionuclide is fixed to values that are customarily in real data.Hence, these data simulate a realistic setting to test the proposed unmixing methods. As described in (15), we simulate the measured spectra with the simulated spectral signatures $\mathbf{\Phi}$ and a background radiation spectrum $\boldsymbol{b}$. After fixing the mixing

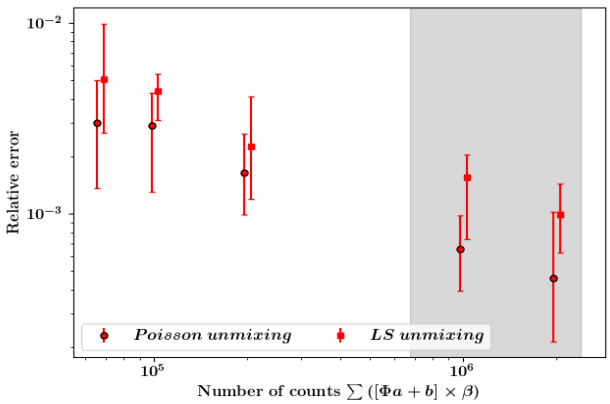

(a) Estimation of ^{7}Be

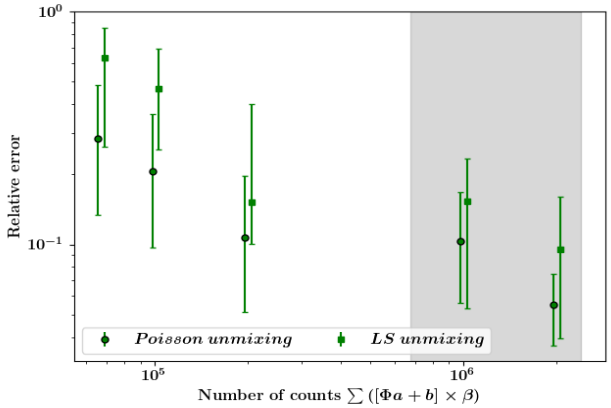

(b) Estimation of ^{22}Na

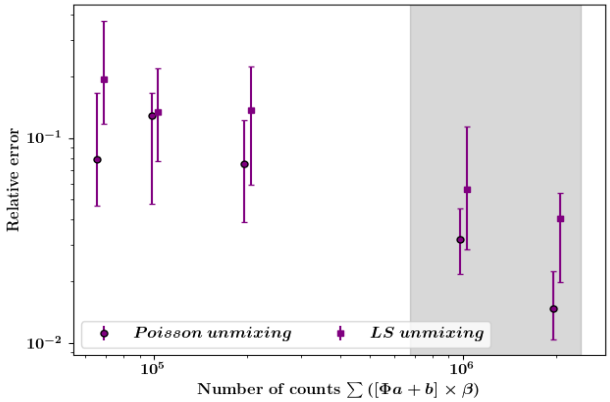

(c) Estimation of ^{40}K

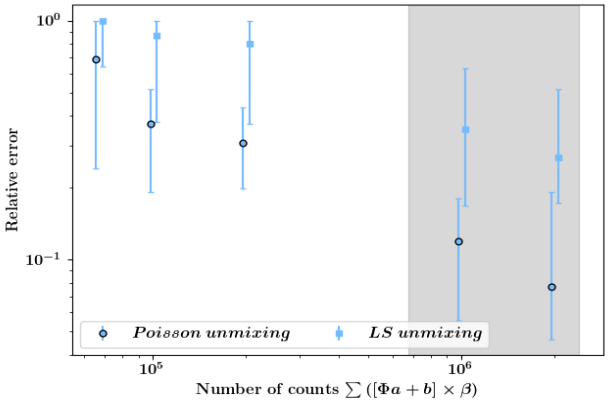

(d) Estimation of ^{137}Cs

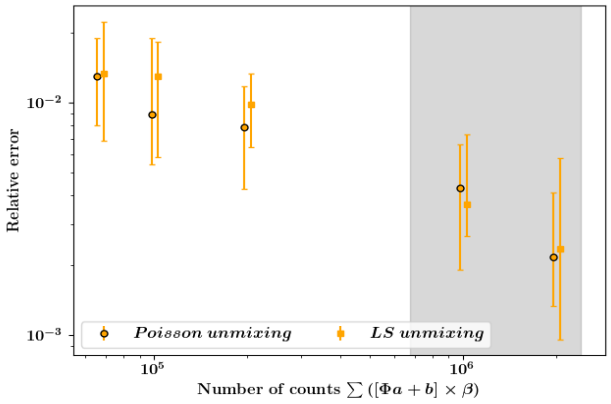

(e) Estimation of ^{210}Pb

Fig. 4: Estimation relative error obtained by Poisson unmixing and LS unmixing, the gray region represents the range of counts numbers in real spectra that we measured for aerosol samples.

weights of each radionuclide $\boldsymbol{a}$, the counting time is changed in the simulation process with a factor β.

$$\boldsymbol{x} \sim \mathcal{P}([\boldsymbol{\Phi a} + \boldsymbol{b}] \times \beta) \tag{15}$$

We generate also 30 simulations for each mixture using random Poisson processes. Next, we apply the least squares unmixing and Poisson unmixing algorithms to the simulated spectra. The estimation performances have been therefore assessed for the 5 radionuclides in Figure 4 with relative error

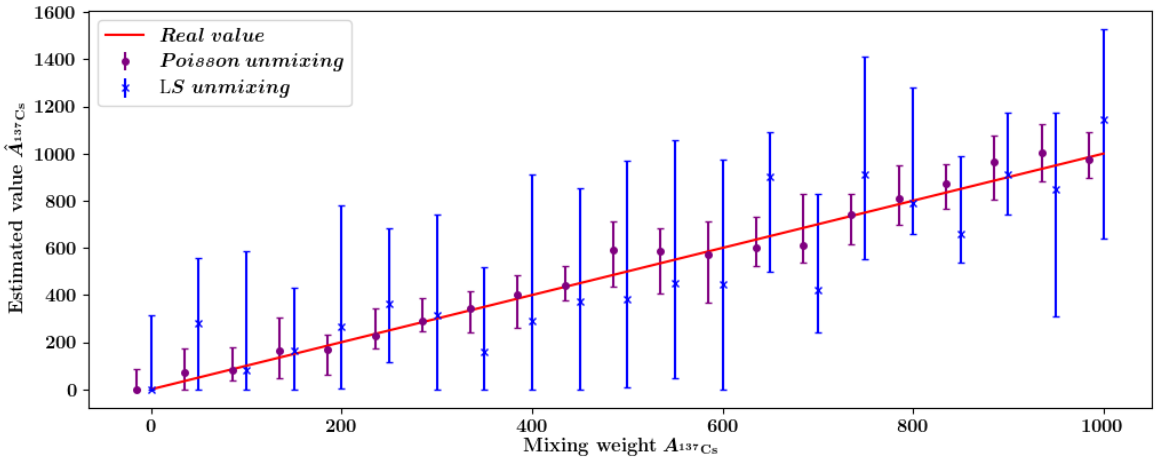

Fig. 5: Estimation of ^{137}Cs in the case that activity levels of other radionuclides and background radiation are fixed. Estimation results for Monte-Carlo simulations are compared to the real values of the mixing weight of ^{137}Cs.

bar defined by $\frac{\|a-\hat{a}\|}{\|a\|}$. The results are illustrated with the median value of Monte-Carlo simulations and the confidence intervals given by percentile 25 and percentile 75.

Results

- Compared to least squares unmixing, we get lower relative errors with the Poisson unmixing for ^{7}Be, ^{22}Na, ^{40}K and ^{137}Cs, which are composed of peaks and significant continuum contributions. The results obtained for ^{210}Pb indicate that both estimators have similar performances for estimating a spectrum which consists of dominant peak.

- With respect to the number of counts carried out by the factor β, the realistic levels in experimental measurements are illustrated in gray regions of Figure 4. The analysis shows the advantage of Poisson unmixing in the task of activity estimation in the environmental samples.

As mentioned previously, the activity estimation at low statistics is a difficult problem to handle in the spectral analysis. We evaluate more precisely the estimation of the low-activity radionuclide ^{137}Cs. For this purpose, we perform a scenario of simulations with 5 radionuclides described at the beginning of this section, the counting rate of ^{137}Cs ranges from 0 to a realistic level in practice. Figure 5 plots the estimation performance of ^{137}Cs while the mixing weights of other radionuclides are fixed. The results demonstrate that the Poisson unmixing improves the estimation performance for low-activity source.
The results shown in this section with simulated data confirm the good performance of using spectral unmixing approach. Further experiments on real spectra will be performed in the next section.

IV. Experimental results with real spectra from aerosol samples' measurements

In this section, we aim to validate the proposed approaches for real data. We focus on the measurement of aerosol samples which is a part of the surveillance network in the laboratory. In the framework of the radiological environmental monitoring program in France or for research purpose in radioecology, we are concerned with measuring levels of radioactivity in environmental samples. In France, ^{137}Cs is an artificial radionuclide present in the environment due to the global fallout (atmospheric nuclear weapon tests and Chernobyl accident) and in the air due to resuspension phenomenon. The aerosol filters are collected weekly by the 10 high flow (800 m^3.h^{-1}) air samplers of the OPERA-Air network. Their volume higher than 120 000 m^3 enables to determine the ^{137}Cs activity concentration in the air at trace level around 0.1 μBq.m^{-3}.
It is well known that rapid detection of artificial radionuclides is mandatory for emergency preparedness. In practice, we detect the presence of ^{137}Cs from the measurement of an aerosol sample more than one week after the sampling. It is of interest to evaluate the different approaches with short-time counting statistics. For this purpose, a scenario of measurements is performed in the laboratory with an aerosol sample. These measurements are performed half an hour after the sampling in a continuous manner with defined counting times for 8 days. The progressive measurements are described in Table. I. These measured spectra are subsequently analyzed with proposed spectral unmixing algorithms and Genie2000 used in the laboratory. Since spectral signatures are required for the spectral unmixing algorithms, a spectral library is simulated for the detector and geometry used in this experiment.
The contribution of this section is as follows: firstly, we discuss the choice of spectral signatures since the subset of active radionuclides is unknown in practice. Next, the results are compared with those performed with Genie2000.

TABLE I: Successive measurements with increasing counting times carried out on an aerosol filter sampled on 19/04/2019 8:46:00

	Start time	Counting time(s)
s1	19/04/2018 09:10:53	1800
s2	19/04/2018 09:41:42	1800
s3	19/04/2018 10:12:30	1800
s4	19/04/2018 10:44:11	3600
s5	19/04/2018 11:45:03	3600
s6	19/04/2018 12:46:59	5400
s7	19/04/2018 14:20:23	10800
s8	19/04/2018 17:22:17	54000
s9	20/04/2018 08:41:41	28000
s10	20/04/2018 16:29:59	240000
s11	23/04/2018 11:44:44	320000

A. Dimension of spectral library

As discussed in the previous section, the spectral unmixing process aims to estimate the mixing weights of spectral signatures. However, finding the optimal subset of spectral signatures is important to estimate mixing weights more accurately. In the context of this experiment, it is well known that we can detect several short-lived radionuclides after the sampling, which decay very fast as time goes on. Accordingly, the first measurement (Figure 6-a) contains more contributions comparing to the last measurement (Figure 6-b). The last measurement Figure 6-b corresponds to a routine aerosol measurement: the predominant peak at 477 keV is characteristic of ^{7}Be, a cosmic-ray induced radionuclide. It gives also rise to the Compton continuum from 165 to 313 keV. Other peaks enable to identify and quantify other natural radionuclides: ^{40}K at 1460 keV or ^{210}Pb at 46 keV. ^{137}Cs and ^{22}Na can also be determined at trace level thanks to their respective peak at 662 keV and 1274 keV.

Consequently, the real subset of active spectral signatures for each measurement is different. In order to study the impact of the dimension of the spectral library when we use spectral unmixing estimators, we apply the two algorithms with spectral signatures according to:

- ^{7}Be, ^{22}Na, ^{40}K, ^{137}Cs, ^{210}Pb, so that the measured spectra are supposed to be separated to these 5 radionuclides: $\mathbf{\Phi^5} = [\phi_1, ...\phi_5]$.
- ^{7}Be, ^{22}Na, ^{40}K, ^{137}Cs, ^{210}Pb, ^{208}Tl, ^{212}Bi, ^{212}Pb, ^{214}Bi, ^{214}Pb, with respect to $\mathbf{\Phi^{10}} = [\phi_1, ...\phi_{10}]$.

As results, Figure.7 illustrates the estimated mixing weights for the 11 measured spectra with both strategies for spectral signatures choice. Comparing both experiments, we get more stable estimated values with $\mathbf{\Phi^{10}} = [\phi_1, ...\phi_{10}]$. However, in the case of $\mathbf{\Phi^5} = [\phi_1, ...\phi_5]$, the estimated values we obtained with the two estimators converge in the last measurement.
More specifically, as discussed in other spectral unmixing applications, badly chosen spectral signatures can introduce a bias on the estimation. To confirm this assumption, quantitative analysis with simulations have been carried out as described in (15). Spectra s1 $\rightarrow$ s11 have been simulated with similar activity levels than the measurements. Considering the mixing weights of ^{7}Be, ^{22}Na, ^{40}K, ^{137}Cs, ^{210}Pb as constants, we simulate other natural radionuclides with realistic decreasing levels. Figure 8 compares the estimation performance of these 5 natural radionuclides using $\mathbf{\Phi^5} = [\phi_1, ...\phi_5]$ and $\mathbf{\Phi^{10}} = [\phi_1, ...\phi_{10}]$ for simulated spectra.

Results

- As shown in the first column of Figure 8, by using $\mathbf{\Phi^5} = [\phi_1, ...\phi_5]$ to unmix spectra in which other radionuclides decay quickly, the spectral unmixing provides bias in the first measurements.
  - For ^{7}Be, ^{22}Na and ^{40}K (respectively Figure 8-a,c,e), Poisson unmixing tends to over-estimate the activities with respect to the least squares unmixing. Statistically the Poisson unmixing is more sensitive to the choice of spectral library. The reason is, firstly, the logarithmic scaling in the likelihood term introduces more significant residual errors (^{7}Be at high activity levels), secondly, Poisson unmixing aims to precisely fit the measured spectrum with the full spectrum (^{22}Na and ^{40}K with significant continuum contributions).
  - The ^{137}Cs(Figure 8-g)impacted by continua of other radionuclides and present at low activity level is more overestimated by least squares unmixing.
  - The estimation of ^{210}Pb (Figure 8-i]) which is dominated by the peak, is less impacted by the spectral library.
- The results obtained with a more complex spectral library $\mathbf{\Phi^{10}} = [\phi_1, ...\phi_{10}]$ are shown in the second column of Figure 8. The estimation is more accurate with this second strategy.

In summary, we obtained similar results than those for real spectra. It highlights that the accurate identification of spectral signatures is the precondition for the spectral unmixing.

B. Comparisons with peak calculation analysis

We compare the results of the proposed spectral unmixing estimators with those of Genie2000 used in the laboratory. As discussed previously, we use the results obtained with spectral signatures in dimension of 10, which is more suitable for spectral unmixing of the measured spectra. We focus on the results of the 5 concerning radionuclides and two natural radionuclides ^{212}Bi and ^{214}Bi. The estimated values are compared in Figure 9 and Figure 10.

Results

- Figure 9-a,b,c,d show the results for ^{7}Be, ^{22}Na, ^{40}K, ^{210}Pb. At the end of the measurements, the mixing weights estimated by Poisson unmixing and LS unmxing are closed to those obtained with Genie2000. This is motivated by the sufficient counting rate obtained with the last measurement during 4 days (as shown in the inset of each figure).

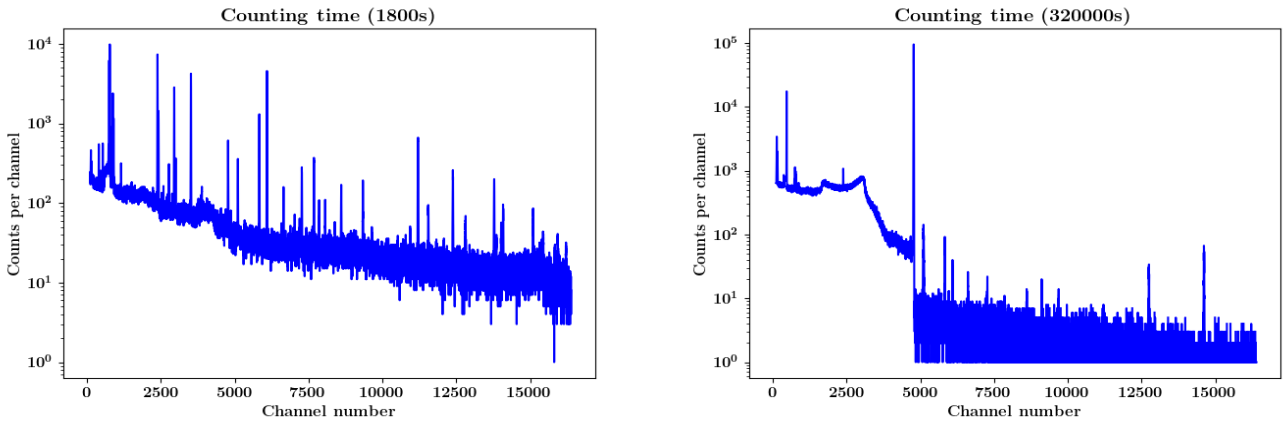

(a) spectrum s1

(b) spectrum s11

Fig. 6: Measured spectra for s1 and s11

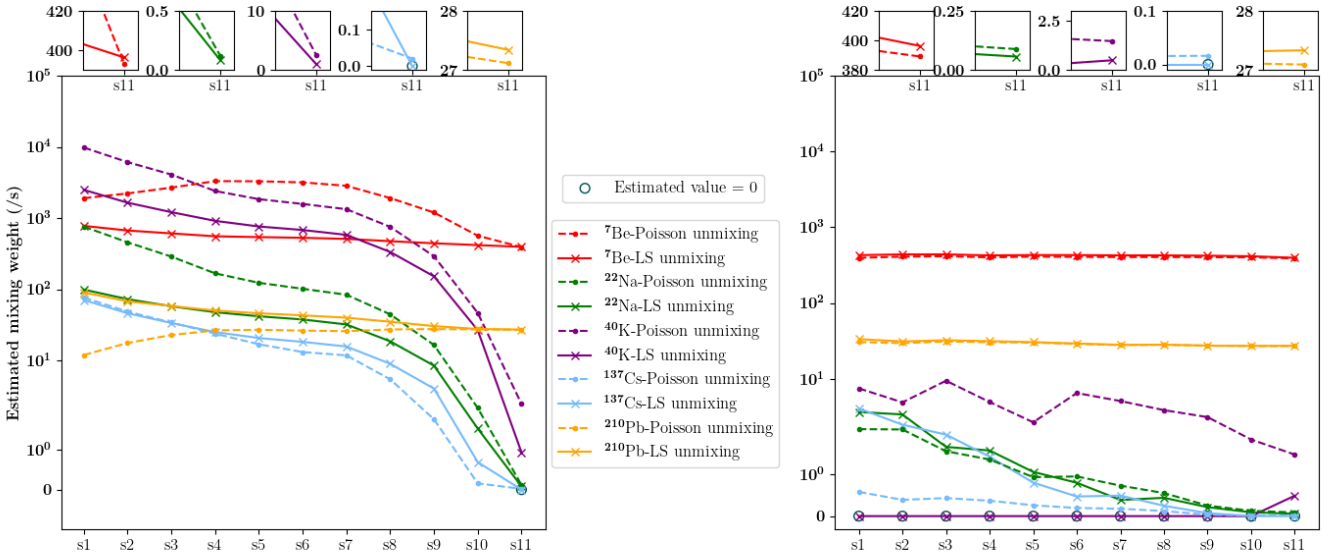

Fig. 7: The estimated mixing weights for each measured spectrum($\mathbf{\Phi^5} = [\phi_1, ...\phi_5]$ on the left, $\mathbf{\Phi^{10}} = [\phi_1, ...\phi_{10}]$ on the right). Results for the last measurement are presented in the top of the figures.

- As shown in Figure 9-e,f, the activity of short-lived radionuclides decreases in the first two days after the sampling. This is confirmed by the similar results obtained with three estimators.

- Figure 10 indicates that, the ^{137}Cs has not been detected in the end of the measurements with least squares unmixing. Contrarily, we obtain similar estimated values with Poisson unmixing and Genie2000. This may be motivated by a bias introduced by the background spectrum, since at low statistics, the least squares unmixing introduces a peak as a false peak in the background spectrum. The analysis shows that, ^{137}Cs , present at the lowest activity level, is identified and quantified with Poisson unmixing algorithm four days before the usual method Genie2000.

In this section, we can conclude from the experiments on real measurements that, firstly, for spectral unmixing estimators, the lack of knowledge of active radionuclides leads to under-fitting or over-fitting the model which introduce a bias to the results. Secondly, Poisson unmixing yields significant improvement for estimating radioactivity, especially when the counting rate is low, which is a key advantage for the rapid detection of anomaly in the air.

V. CONCLUSION

We present in this paper activity estimation algorithms based on spectral unmixing, which exploit the full spectrum of radionuclides and introduce the measured spectrum with pure spectral signatures known in advance. We formulate the spectral unmixing problem by inverse problem to estimate mixing weights of each radionuclide in the measured spectrum. We propose two estimators: least squares regression

approach using FISTA algorithm and Poisson unmixing based on Poisson statistics using Primal-dual algorithm.
Results on simulated and real spectra provide good performance with the least squares unmixing and the Poisson unmixing. The latter which precisely takes into account the Poisson statistics of the physical process underlying the detection, presents significant advantages when the counting rate is low. In the context of rapid detection which leads to measuring low level activity in environmental samples, an important advantage is that the time for detection and identification has been reduced for artificial radionuclides.
The discussion in section IV concerning the problem of spectral library dimension emphasizes the importance of using an optimal spectral library with spectral unmixing estimators. This opens perspectives on estimating jointly the set of active radionuclides: the aim is to select in the complex spectral library, the smallest number of radionuclides that best fit the measured spectrum.

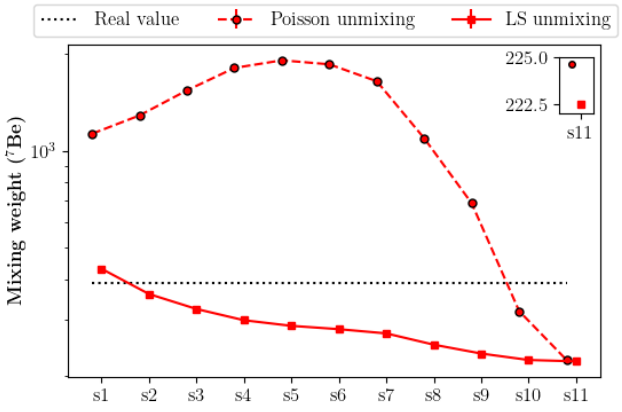

(a) Estimation of ^{7}Be with $\mathbf{\Phi^5}$

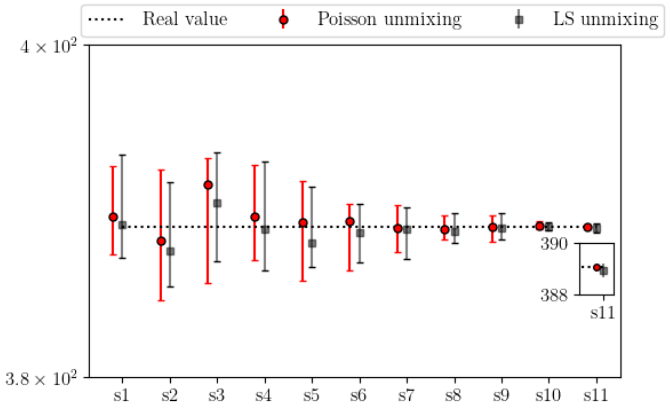

(b) Estimation of ^{7}Be with $\mathbf{\Phi^{10}}$

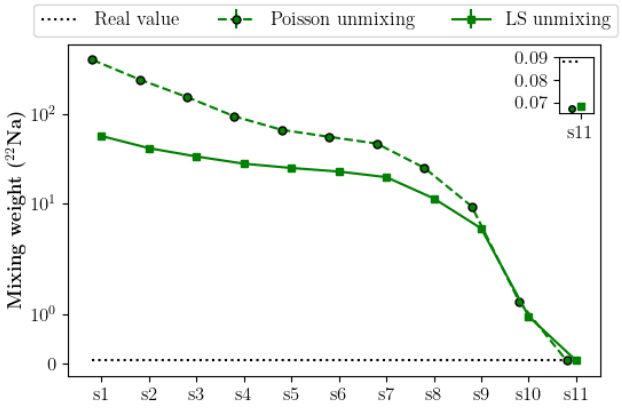

(c) Estimation of ^{22}Na with $\mathbf{\Phi^5}$

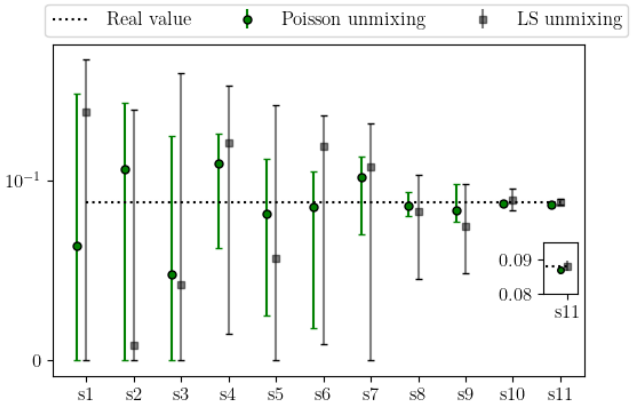

(d) Estimation of ^{22}Na with $\mathbf{\Phi^{10}}$

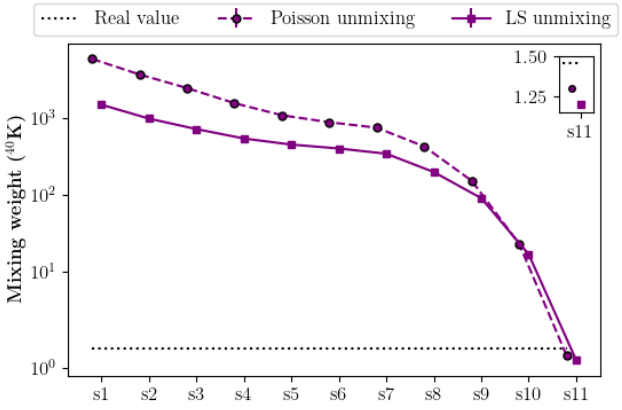

(e) Estimation of ^{40}K with $\mathbf{\Phi^5}$

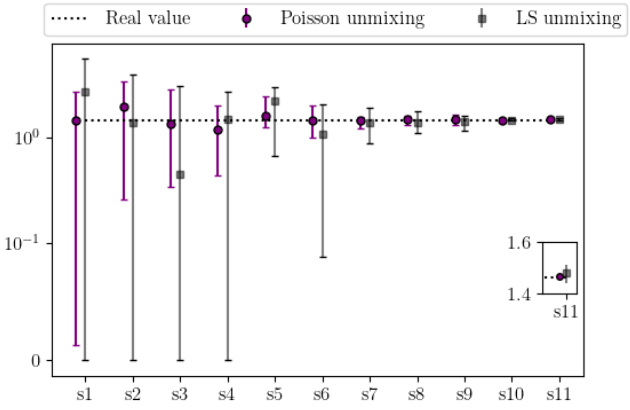

(f) Estimation of ^{40}K with $\mathbf{\Phi^{10}}$

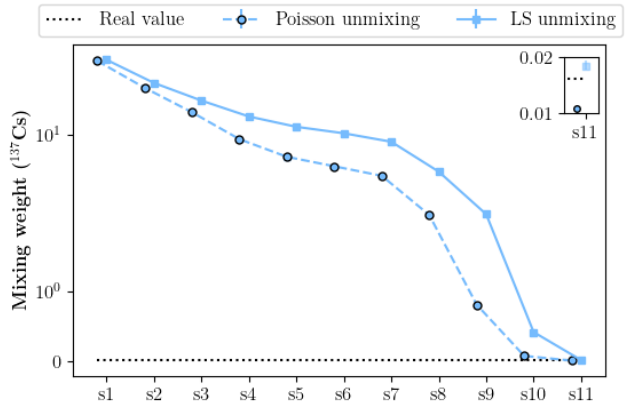

(g) Estimation of ^{137}Cs with $\mathbf{\Phi^5}$

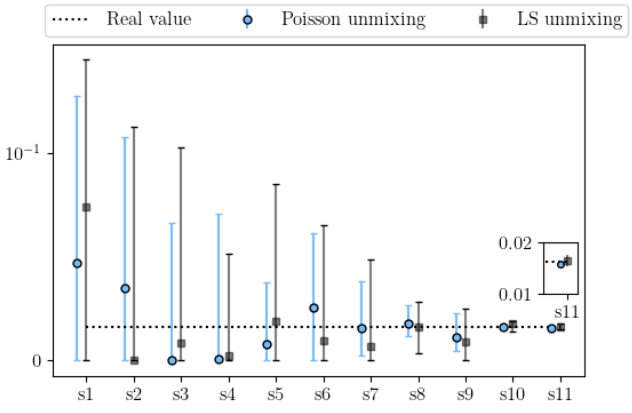

(h) Estimation of ^{137}Cs with $\mathbf{\Phi^{10}}$

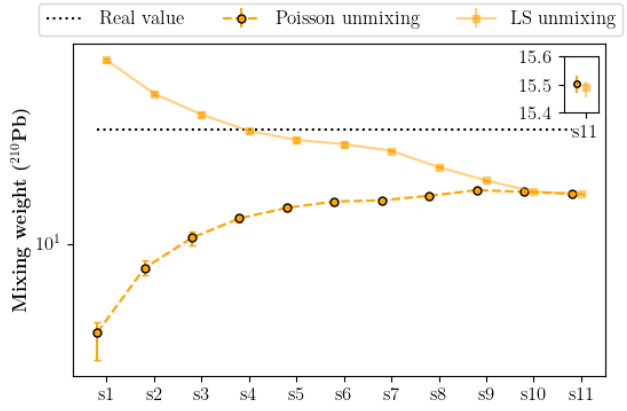

(i) Estimation of ^{210}Pb with $\mathbf{\Phi^5}$

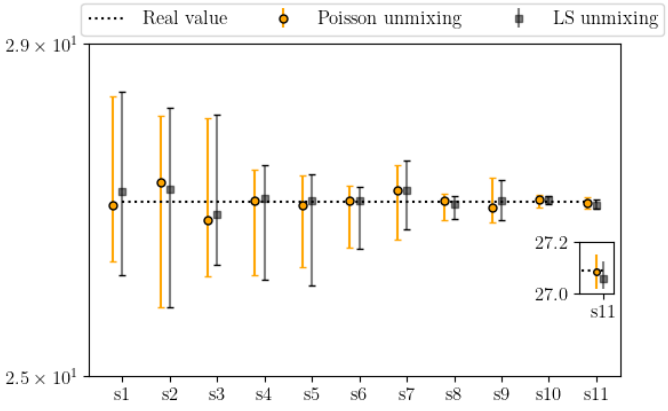

(j) Estimation of ^{210}Pb with $\mathbf{\Phi^{10}}$

Fig. 8: Results on simulations with similar activity levels of the real spectra for $s1 \rightarrow s11$. The first column according to spectral signatures $\mathbf{\Phi^5} = [\phi_1, ...\phi_5]$, the second column according to $\mathbf{\Phi^{10}} = [\phi_1, ...\phi_{10}]$. The estimated mixing weights are compared to real values for the 11 spectra and the results of $s11$ on the right of each figure.

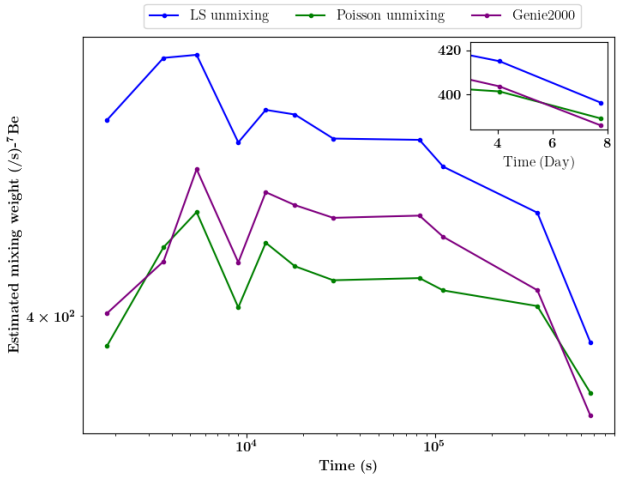

(a)

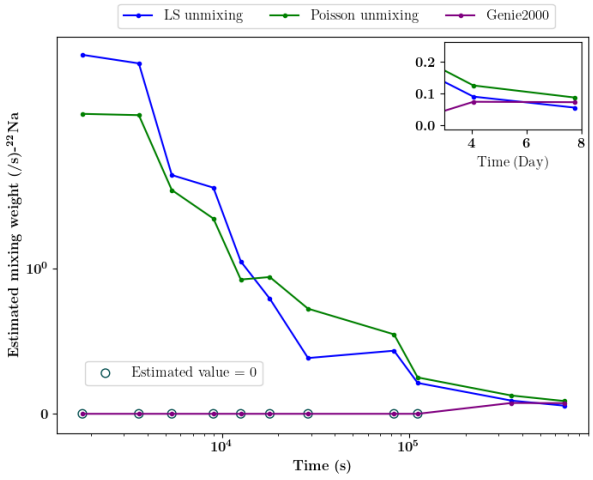

(b)

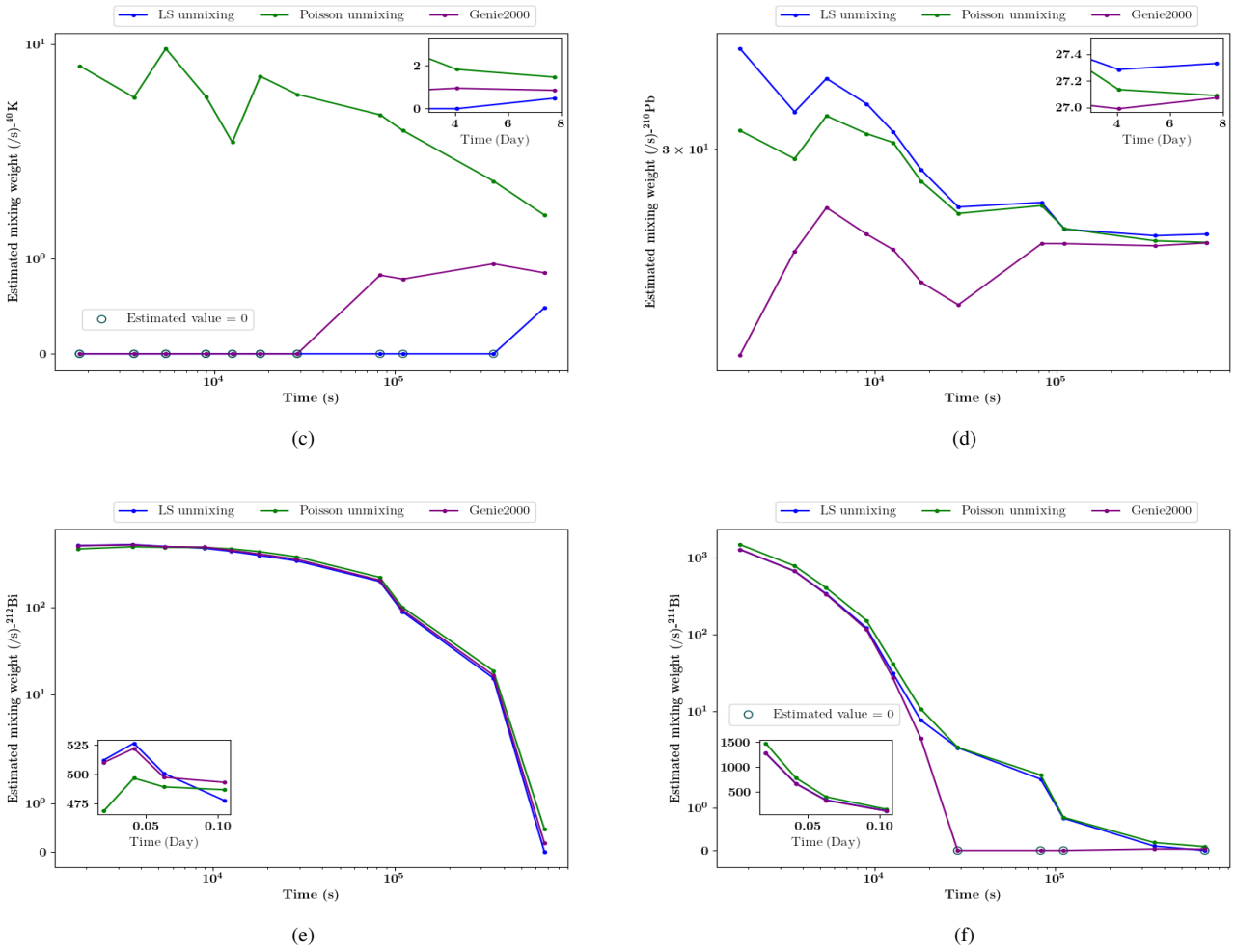

Fig. 9: The results obtained by net peak area analysis of Genie2000 are converted to mixing weights by $\boldsymbol{a}_i = \frac{{S_{net}}^i}{{S_{net}}^{\phi_i}}$ (${S_{net}}^i$: the measured net area of ith radionuclide, ${S_{net}}^{\phi_i}$: the net area of ith spectral signature). The results are plotted as a function of the ending time of each measurement.

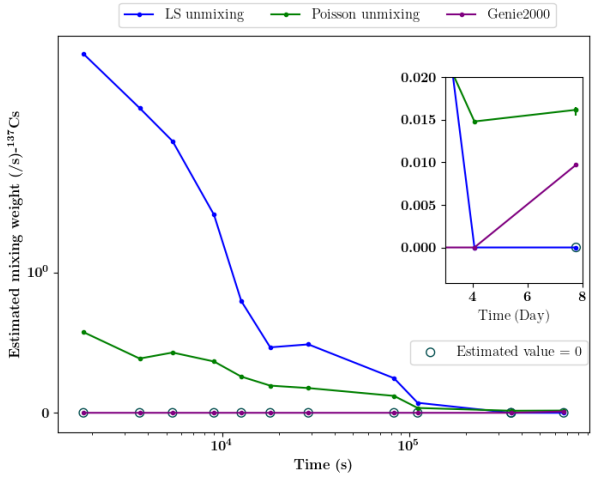

Fig. 10: Estimation of ^{137}Cs. The least squares unmixing provides zero as mixing weight for ^{137}Cs at the end of the measurements. The estimated value obtained by Poisson unmixing is presented with error bar that we obtained in the simulations.

REFERENCES

[1] A. de Vismes Ott, R. Gurriaran, X. Cagnat, and O. Masson, "Fission product activity ratios measured at trace level over france during the fukushima accident," *Journal of Environmental Radioactivity*, vol. 125, pp. 6–16, Nov 2013.

[2] G. F. Knoll, *Radiation Detection and Measurement*, 4th ed. John Wiley & Sons, 2010.

[3] G. Gilmore, *Practical Gamma-ray Spectrometry*, 2nd ed. Wiley-Blackwell, 2001.

[4] J. M. Kirkpatrick and B. M. Young, "Poisson statistical methods for the analysis of low-count gamma spectra," *IEEE Transactions on Nuclear Science*, vol. 56, no. 3, pp. 1278–1282, Jun 2009.

[5] P. Hendriks, J. Limburg, and R. de Meijer, "Full-spectrum analysis of natural γ-ray spectra," *Journal of Environmental Radioactivity*, vol. 53, no. 3, pp. 365–380, Apr 2001.

[6] Y. Sepulcre, T. Trigano, and Y. Ritov, "Sparse regression algorithm for activity estimation in γ spectrometry," *IEEE Transactions on Signal Processing*, vol. 61, no. 17, pp. 4347–4359, Sep 2013.

[7] E. Yoshida, K. Shizuma, S. Endo, and T. Oka, "Application of neural networks for the analysis of gamma-ray spectra measured with a ge spectrometer," *Nuclear Instruments and Methods in Physics Research Section A Accelerators Spectrometers Detectors and Associated Equipment*, vol. 484, no. 1-3, pp. 557–563, May 2002.

[8] S. Sharma, C. Bellinger, N. Japkowicz, R. Berg, and K. Ungar, "Anomaly detection in gamma ray spectra: A machine learning perspective," pp. 1–8, 07 2012.

[9] N. Keshava and J. F. Mustard, "Spectral unmixing," *IEEE Signal Process. Mag.*, vol. 19, no. 1, pp. 44–57, Jan 2002.

[10] M.-D. Iordache, J. M. Bioucas-Dias, and A. Plaza, "Sparse unmixing of hyperspectral data," *IEEE Transactions on Geoscience and Remote Sensing*, vol. 49, no. 6, pp. 2014–2039, Jun 2011.

[11] N. Parikh and S. P. Boyd, "Proximal algorithms," *Foundations and Trends in Optimization*, vol. 1, no. 3, pp. 127–239, 2014.

[12] P. L. Combettes and V. Wajs, "Signal recovery by proximal forward-backward splitting," *SIAM Journal on Multiscale Modeling and Simulation: A SIAM Interdisciplinary Journal*, vol. 4, pp. 1164–1200, 2005.

[13] A. Beck and M. Teboulle, "A fast iterative shrinkage-thresholding algorithm for linear inverse problems," vol. 2, pp. 183 – 202, 2009.

[14] A. Chambolle and T. Pock, "A first-order primal-dual algorithm for convex problems withapplications to imaging," *Journal of Mathematical Imaging and Vision*, vol. 40, no. 1, pp. 120–145, May 2011.

[15] J. F. Briesmeister, "MCNP: A General Monte Carlo N-Particle Transport Code," 2000.

[16] A. Berlizov, *MCNP-CP: A Correlated Particle Radiation Source Extension of a General Purpose Monte Carlo N-Particle Transport Code*, 11 2006, vol. 945.